

The Crystal Structure of a RAS (N-CH₃-2-NH₂-5-Cl-Py)(TCNQ)(CH₃CN) Solvate

T. N. Starodub^{a,*}, D. Fenske^{b,c,d}, O. Fuhr^{c,d}, O. N. Kazheva^e, and V. A. Starodub^a

^aInstitute of Chemistry, Jan Kochanowski University, Kielce, 25-405 Poland

^bInstitute of Inorganic Chemistry Karlsruhe Institute of Technology (KIT), Karlsruhe, 76131 Germany

^cInstitute of Nanotechnology (INT) and Karlsruhe Nano Micro Facility (KNMF) Karlsruhe Institute of Technology (KIT), Eggenstein-Leopoldshafen 76344, Germany

^dLehn-Institute for Functional Materials School of Chemistry and Chemical Engineering Sun Yat-Sen University, Guangzhou, China

^eInstitute of Problems of Chemical Physics, Russian Academy of Sciences, Chernogolovka, Moscow oblast, 142432 Russia

* e-mail: starodub@ujk.edu.pl

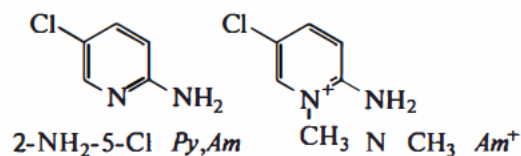
Received March 14, 2019; revised March 14, 2019; accepted May 22, 2019

Abstract—The structure of the radical anion salt (RAS) of 7,7,8,8-tetracyanodimethane (TCNQ) with a cation based on 2-amin-5-chloro-pyridine (2-NH₂-5-Cl-Py, Am), that is, (N-CH₃-2-NH₂-5-Cl-Py)(TCNQ)(CH₃CN), (**1**) is presented. Unlike most TCNQ RASs, which contain flat TCNQ particle stacks, RAS **1** contains practically isolated (TCNQ)₂²⁻ π-dimers with unusually short distances between the planes in the dimers: 3.24 Å. In the RAS **1** IR spectra special features are observed that correspond to the vibronic interactions of molecular vibrations.

1. INTRODUCTION

Creation of multifunctional organic materials is a promising modern trend of micro- and nano-electronics. It is promising to use radical anion salts (RASs) of 7,7,8,8-tetracyanoquinodimethane (TCNQ) with cations that are able to form hydrogen bonds with anion radicals [1]. The presence of such bonds allows formation of channels for indirect magnetic exchange and materials. In our work [2] the (N-Me-2-NH₂-Pz)(TCNQ)₂ salt (Pz is pyrazine) was described, which contains a cation that is able to form hydrogen bonds. However, in this case amino groups of cations of (N-Me-2-NH₂-Pz)⁺ form hydrogen bonds with the non-quaternized atoms of nitrogen of a nearby cation rather than with the atoms of nitrogen of anion-radicals, thus forming dimeric cations (Fig. 1).

Here, we report the synthesis of an RAS with a cation on the basis of 2-amino-5-chloropyridine (2-NH₂-5-Cl-Py, Am):



In this case it is more likely to expect formation of hydrogen bonds between N-CH₃-Am⁺ cations and TCNQ^{•-} radical anions.

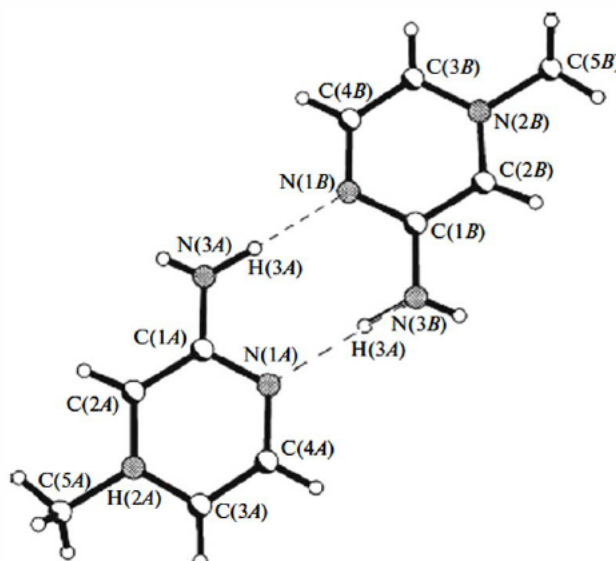


Fig. 1. The cation dimerized (N-Me-2-NH₂-Pz)₂²⁺ in the structure RAS (N-Me-2-NH₂-Pz)(TCNQ)₂.

Table 1. Selected bond distances (Å) and bond angles (deg)

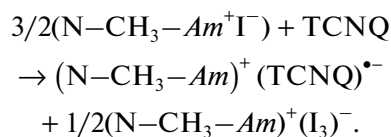
C11–C5	1.728(2)	C16–C18	1.410(3)
N1–C2	1.357(2)	C16–C17	1.420(2)
N1–C6	1.369(2)	N7–C19	1.135(3)
N1–C1	1.469(3)	C19–C20	1.445(3)
N2–C2	1.326(2)	C2–N1–C6	121.1(2)
C6–C5	1.352(3)	C2–N1–C1	119.5(1)
C5–C4	1.407(3)	C6–N1–C1	119.4(1)
C4–C3	1.356(3)	C5–C6–N1	121.0(2)
C3–C2	1.416(3)	C6–C5–C4	119.5(2)
N3–C14	1.153(2)	C6–C5–C11	120.0(1)
N4–C15	1.150(2)	C4–C5–C11	120.4(1)
N5–C17	1.155(2)	C3–C4–C5	119.4(2)
N6–C18	1.157(3)	C4–C3–C2	120.5(2)
C7–C13	1.413(3)	N2–C2–N1	119.9(2)
C7–C12	1.420(2)	N2–C2–C3	121.6(2)
C7–C8	1.422(2)	N1–C2–C3	118.5(2)
C8–C9	1.357(3)	C13–C7–C12	121.6(2)
C9–C10	1.427(2)	C13–C7–C8	121.2(1)
C10–C16	1.412(2)	C12–C7–C8	117.2(2)
C10–C11	1.417(2)	C9–C8–C7	121.7(2)
C11–C12	1.364(3)	C8–C9–C10	121.1(2)
C13–C14	1.413(3)	C16–C10–C11	121.6(1)
C13–C15	1.422(2)	C16–C10–C9	121.1(2)
C11–C10–C9	117.3(2)	N4–C15–C13	178.5(2)
C12–C11–C10	121.5(2)	C18–C16–C10	120.9(1)
C11–C12–C7	121.2(2)	C18–C16–C17	117.1(2)
C14–C13–C7	122.0(1)	C10–C16–C17	121.8(2)
C14–C13–C15	116.3(2)	N5–C17–C16	178.9(2)
C7–C13–C15	121.6(2)	N6–C18–C16	177.9(2)
N3–C14–C13	179.1(2)	N7–C19–C20	178.9(2)

2. MATERIALS AND METHODS

2.1. Synthesis and Crystallization

The *Am* amine was dissolved in methyl iodide and the solution was agitated with a magnetic stirrer until amine iodide (N–CH₃–*Am*⁺)I[–] precipitated. The yield in terms of the amine was 100%.

The RASs were synthesized by the reaction:



RAS precipitates were filtered, washed with ether and hexane, and dried under a vacuum. Recrystallization from acetonitrile was used in order to grow single crystals and for purification. Black–violet needle

shaped crystals with lengths up to 5 mm were obtained. This gave the compound in a 55% yield.

Elemental analysis of the synthesized radical anion salts was performed on a VarioMICRO Superuser analyzer, which gave calc. C, 62.16%; N, 24.16%; H, 3.48%; and Cl, 10.19%; we found C, 62.31%; N, 24.21%; H, 3.57%; and Cl, 10.23%.

RAS compositions were determined spectrophotometrically, as described in [3]. This corresponds to the formula (N–CH₃–*Am*)⁺(TCNQ)^{•–} (**I**).

2.2. IR Spectra

The infrared absorption spectra of the powdered (**I**) samples were recorded in the frequency range from 600 to 4000 cm^{–1} at room temperature with a Thermo Scientific Nicolet IS10 spectrometer with a Smart MIRacle attachment.

2.3. Determination of the Single-Crystal Structure

An X-ray diffraction study of (**I**) was carried out with a StadiVari diffractometer at 180 K (CuK_α-radiation, multilayer optics, and the rotation method). STOE X-Red32 empirical absorption corrections of the experimental intensities were applied, with absorption correction by Gaussian integration, analogous to that of P. Coppens in “The Evaluation of Absorption and Extinction in Single-Crystal Structure Analysis” in [4]. Scaling of reflection intensities was then performed within STOE LANA [5]. Finally, spherical absorption correction was performed within STOE LANA. The structures were solved by direct methods followed by Fourier difference syntheses using SHELXS-97 software [6] and refined by the full-matrix least-squares method in an anisotropic (isotropic for H atoms) approximation for all non-hydrogen atoms using SHELXL-97 software [7].

The basic crystallographic and experimental data are as follows: C₂₀H₁₅ClN₇, *M* = 388.84, monoclinic, *P*2₁/*c*, *a* = 9.2556(4) Å, *b* = 16.8791(6) Å, *c* = 13.0972(5) Å, β = 106.804(3)°, *V* = 1958.7(1) Å³, *Z* = 4, *D*_x = 1.32 g cm^{–3}, μ = 1.891 mm^{–1}, (2θ)_{max} = 137.02°, quantity of measured reflections 7945, independent reflections 3004, 314 parameters used in refinement, range of *h*, *k*, *l*: –10 → *h* → 10, –19 → *k* → 12, –14 → *l* → 15, *R* = 0.046 for 2691 reflections with [*F*₀ > 4σ(*F*₀)]. The bond lengths and angles are listed in Table 1.

The crystallographic data have been deposited to the Cambridge Crystallographic Data Centre (CCDC-1850699). Copies of the data can be obtained free of charge from The Director, CCDC, 12, Union Road, Cambridge CB2 1EZ, UK (fax: +44 1223 336033; e-mail: deposit@ccdc.cam.ac.uk or http://www.ccdc.cam.ac.uk).

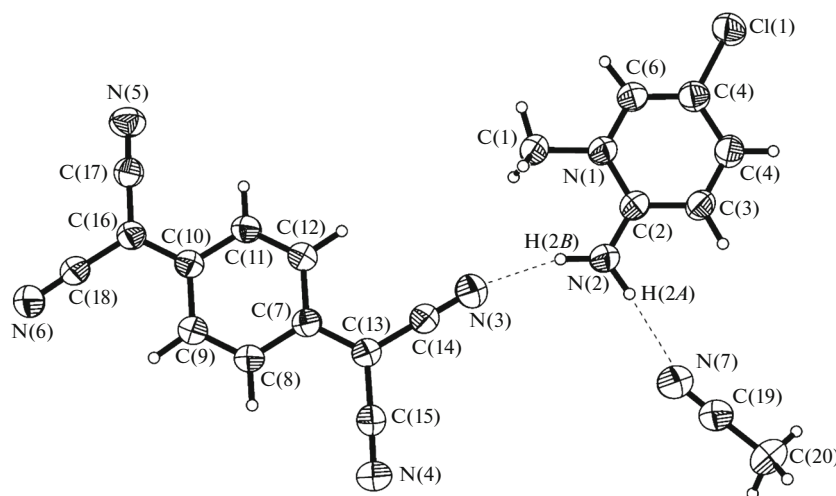


Fig. 2. The structure and hydrogen interactions between the radical anion, cation, and a molecule of acetonitrile in (I) (displacement ellipsoids are drawn at the 50% probability level).

3. RESULTS AND DISCUSSION

The crystalline structure of RAS (1) is formed by the $\text{TCNQ}^{\bullet-}$ radical anion, the $(\text{N}-\text{CH}_3\text{-2-NH}_2\text{-5-Cl-Py})^+$ cation, and the acetonitrile solvent molecule, which are located in general positions of the unit cell. One peculiarity of the crystal structure is the intermolecular bifurcational H interactions with the participation of the amino group of the cation according to the following parameters: $\text{N}(2)\cdots\text{N}(3)$ 2.899(3) Å, $\text{N}(3)\cdots\text{H}(2B)$ 2.04(2) Å, $\text{N}(2)\text{-H}(2B)\cdots\text{N}(3)$ 163(2)°, $\text{N}(2)\cdots\text{N}(7)$ 3.009(3) Å, $\text{N}(7)\cdots\text{H}(2A)$ 2.12(2) Å, $\text{N}(2)\text{-H}(2A)\cdots\text{N}(7)$ 173(2)° (the sums of the Van der Waals radii are: $\text{N}\cdots\text{N}$ 3.10 Å, $\text{N}\cdots\text{H}$ 2.75 Å [8]) (Fig. 2). The geometry of the radical anion and cation is maximally close to co-planar: the maximum deviations of atoms out of the corresponding average planes drawn through all non-hydrogen atoms of the molecules are 0.07 Å (atom N(3)) and 0.01 Å (atom Cl(1)), accordingly.

Moreover, presumably, it is possible to discuss a substantial degree of supramolecular conjugation between the cation and radical anion, that is, the maximum deviation of non-hydrogen atoms out of the average plane drawn through all non-hydrogen atoms of both cations and radical anions does not exceed 0.27 Å (atom C(1)), while the dihedral angle between the planes of these molecules is equal to 172.3°.

On the basis of the molecular structure of TCNQ particles it is possible to define their charge [9, 10], which is within the limits of 0.91–0.95 e/mol. This means the practical absence of donor–acceptor interactions between the $(\text{N}-\text{CH}_3\text{-2-NH}_2\text{-5-Cl-Py})^+$ cation and the radical anion.

The molecules in the structure I are organized in layers (Fig. 3). It is also possible to distinguish mixed columns formed by cations and π -dimers from partly

overlapped radical anions in the structure, as well as molecules of solvent between them. In the dimer the distance between the middle planes of anion radicals is 3.24 Å and the dihedral angle on the symmetry conditions is equal to 0° (Fig. 4). We note that the interplanar spacing in a dimer is the same as in the low temperature phase of ARS of $\text{K}^+(\text{TCNQ})^{\bullet-}$, where, however, the cause of dimerization is Peierls instability of TCNQ columns [11].

We note the formation of unusual $(\text{TCNQ})_2^{2-}$ π -dimers; in most cases such dimers originate between the radical anion and neutral $([\text{TCNQ}]_2^{\bullet-})$ molecule, or σ -dimers with unusually long C–C bonds $([\text{TCNQ}-\text{TCNQ}]^{2-})$ occur [1]. As is obvious from Fig. 3, $(\text{TCNQ})_2^{2-}$ π -dimers are bound in endless chains due to supramolecular bonds with $(\text{N}-\text{CH}_3\text{-2-NH}_2\text{-5-Cl-Py})^+$ cations. Similar structures that are unusual for a TCNQ RAS were discovered in $[\text{Mn}(\text{phen})_3](\text{TCNQ})_2 \cdot \text{H}_2\text{O}$ [12], where $(\text{TCNQ})_2^{2-}$ π -dimers were bound to each other through $[\text{Mn}(\text{phen})_3]^{2+}$ cations. The supramolecular contacts result in anti-ferromagnetism of the RAS [13].

Supramolecular contacts result in lowering the local symmetry of TCNQ from D_{2h} to C_{2h} . This is manifested in the distinction of $\text{C}_{13}\text{-C}_{14}$ and $\text{C}_{16}\text{-C}_{18}$ bond lengths (the inverses are related to each other) and therefore the $\text{C}_{13}\text{-C}_{15}$ and $\text{C}_{16}\text{-C}_{17}$ bond lengths (Table 1); in this case the bonds of the cyan groups that form hydrogen bonds with the amino group of the $(\text{N}-\text{CH}_3\text{-2-NH}_2\text{-5-Cl-Py})^+$ cation are shorter.

Group-theory analysis allows one to classify all 54 normal vibrations of the TCNQ molecule according to the types of symmetries of the D_{2h} group according to the expression:

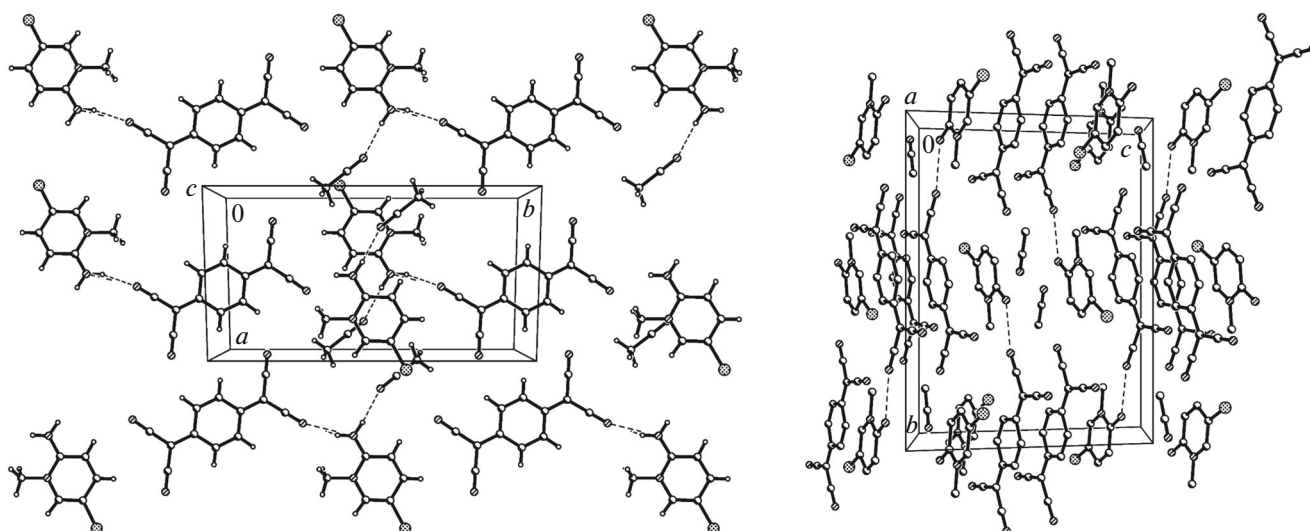


Fig. 3. Fragments of the crystalline structure (I).

$$\Gamma_{54} = 10A_g(\text{R}) \oplus 9B_{1g}(\text{R}) \oplus 5B_{2g}(\text{R}) \\ \oplus 3B_{3g}(\text{R}) \oplus 4A_u(\text{in}) \oplus 5B_{1u}(\text{IR}) \\ \oplus 9B_{2u}(\text{IR}) \oplus 9B_{3u}(\text{IR}),$$

where R means that the oscillation is active in the Raman spectrum; in means that it is inactive in both the Raman spectrum and the IR spectrum; and IR means it is active in the IR spectrum. Thus, in the IR spectrum 23 oscillations are active, antisymmetric in relation to an inversion, while 27 symmetric vibrations are active in the Raman spectrum. Upon lowering the symmetry to C_{2h} the center of inversion is preserved; consequently, the exclusion principle remains in effect. For the C_{2h} group the normal vibrations of a TCNQ particle can be classified based on the types of symmetry according to the expression:

$$\Gamma_{54} = 19A_g(\text{R}) \oplus 9A_u(\text{IR}) \\ \oplus 8B_g(\text{R}) \oplus 18B_u(\text{IR}).$$

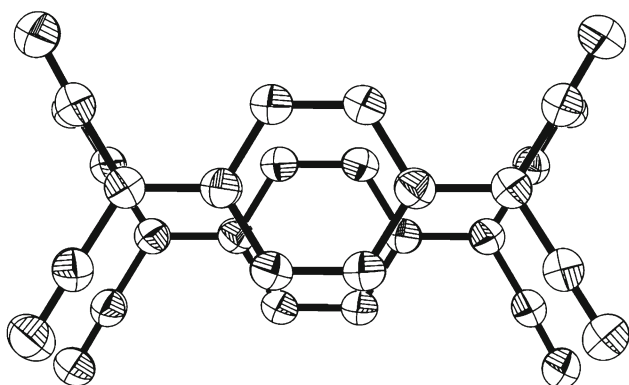


Fig. 4. Overlapping of $\text{TCNQ}^{\bullet-}$ radical anions in a dimer (the hydrogen atoms are omitted for clarity).

In this case there are identical numbers of lines in the IR and Raman spectra, that is, 27 that are symmetric in relation to an inversion in the Raman spectrum and 27 are antisymmetric in the IR spectrum. The IR spectrum of RAS (I) is presented in Fig. 5. The bands observed at 2157 (CN stretch) and 833 cm^{-1} (CH bend) confirm the existence of a negative charge on the $\text{TCNQ}^{\bullet-}$ [14, 15].

The lines of the oscillation structure are observed on the background of continuous absorption, which is characteristic for conducting RASs that contain columns of TCNQ [1, 16]. In addition, as is obvious from Fig. 4, overlap of the lines of the oscillation structure occur at 2157, 1494, 1266, and in the area of $700\text{--}1050\text{ cm}^{-1}$. Taking the absence of TCNQ columns into account, it is possible to explain such features of the IR

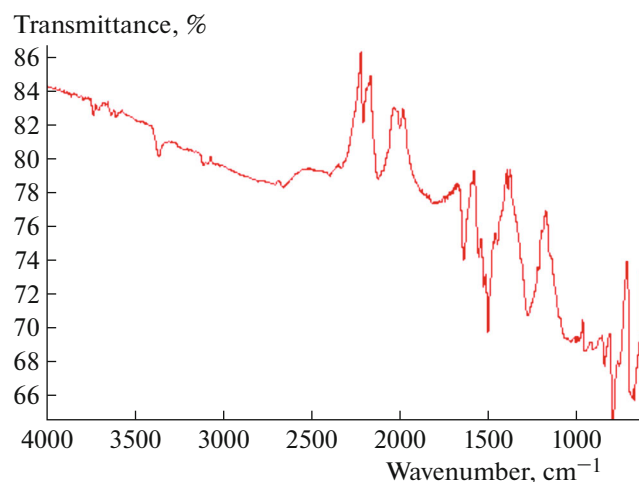


Fig. 5. The IR spectra of the RAS (I).

spectrum by so-called vibronic interactions (the interaction of π -electrons with the molecular vibrations of TCNQ) [17].

As can be seen, the synthesized RAS does not contain TCNQ stacks, which are characteristic of most of the known RAS TCNQs. However, peculiarities occur in the infrared spectrum that are simply explained by the electron—phonon interaction (EPI). Considering the absence of TCNQ stacks, which are necessary for EPI, these peculiarities can be explained by vibronic interactions.

REFERENCES

1. V. A. Starodub and T. N. Starodub, *Russ. Chem. Rev.* **83**, 391 (2014).
<https://doi.org/10.1070/RC2014v083n05ABEH004299>
2. O. N. Kazheva, D. V. Ziolkovskiy, G. G. Alexandrov, A. N. Chekhlov, O. A. Dyachenko, V. A. Starodub, and A. V. Khotkevich, *Synth. Met.* **156**, 1010 (2006).
3. D. V. Ziolkovsky, A. V. Kravchenko, V. A. Starodub, O. N. Kazheva, and A. V. Khotkevich, *Funct. Mater.* **12**, 577 (2005).
4. *Crystallographic Computing*, Ed. by F. R. Ahmed (Munksgaard, Copenhagen, 1970).
5. J. Koziskova, F. Hahn, J. Richter, and J. Kožíšek, *Acta Chim. Slovaca* **9**, 136 (2016).
6. G. M. Sheldrick, *Acta Crystallogr. A* **64**, 112 (2008).
7. G. M. Sheldrick, *Acta Crystallogr. C* **71**, 3 (2015).
8. S. S. Batsanov, *Inorg. Mater.* **37**, 871 (2001).
9. S. Flandrois and D. Chasseau, *Acta Crystallogr. B* **33**, 2744 (1977).
10. T. M. Krygowski, R. Anulewicz, and J. Kruszewski, *Acta Crystallogr. B* **39**, 732 (1983).
11. M. Konno, T. Ishii, and Y. Saito, *Acta Crystallogr. B* **33**, 763 (1977).
12. G. Vasylets, V. A. Starodub, I. Potočňák, B. Barszcz, A. Graja, and H. Metz, *Synt. Met.* **189**, 86 (2014).
13. D. Šoltéssová, G. Vasylets, E. Čížmár, M. Botko, V. Cheranovskii, V. Starodub, and A. Feher, *J. Phys. Chem. Solids* **99**, 182 (2016).
14. B. Lunelli and C. Pecile, *J. Chem. Phys.* **52**, 2375 (1970).
15. M. S. Khatkale and J. P. Devlin, *J. Chem. Phys.* **70**, 1851 (1979).
16. W. Pukacki, M. Pawlak, A. Graja, M. Lequan, and R. M. Lequan, *Inorg. Chem.* **26**, 1328 (1987).
17. C. B. Duke, N. O. Lipari, and L. Pietronero, *Chem. Phys. Lett.* **30**, 415 (1975).